

The Westerly index as complementary indicator of the North Atlantic Oscillation in explaining drought variability across Europe

Sergio M. Vicente-Serrano¹, Ricardo García-Herrera²⁻³, David Barriopedro²⁻³, Cesar Azorin-Molina¹, Juan I. López-Moreno¹, Natalia Martín-Hernández¹, Miquel Tomás-Burguera⁴, Luis Gimeno⁵, Raquel Nieto⁵

¹Instituto Pirenaico de Ecología, Consejo Superior de Investigaciones Científicas (IPE-CSIC), Campus de Aula Dei, P.O. Box 13034, E-50059, Zaragoza, Spain

² Stratospheric and Tropospheric Research and Modelling (STREAM) Group. Dpto. Física de la Tierra, Astronomía y Astrofísica II. Universidad Complutense de Madrid, Spain

³Instituto de Geociencias (IGEO, CSIC, UCM)

⁴Estación Experimental de Aula Dei, Consejo Superior de Investigaciones Científicas (EEAD-CSIC), Zaragoza, Spain

⁵Environmental Physics Laboratory, Universidade de Vigo, Ourense, Spain.

* Corresponding author: svicen@ipe.csic.es

Abstract: This paper analyses the influence of different atmospheric circulation indices on the multi-scalar drought variability across Europe by using the Standardized Precipitation Evapotranspiration Index (SPEI). The monthly circulation indices used in this study include the North Atlantic Oscillation (NAO), the East Atlantic (EA), the Scandinavian (SCAN) and the East Atlantic-Western Russia (EA-WR) patterns, as well as the recently published Westerly Index (WI), defined as the persistence of westerly winds over the eastern north Atlantic region. The results indicate that European drought variability is better explained by the station-based NAO index and the WI than by any other combination of circulation indices. In northern and central Europe the variability of drought severity for different seasons and time-scales is strongly associated with the WI. On the contrary, the influence of the NAO on southern Europe droughts is stronger than that exerted by the WI. The correlation patterns of the NAO and WI with the SPEI show a spatial complementarity in shaping drought variability across Europe. Lagged correlations of the NAO and WI with the SPEI also indicate enough skill of both indices to anticipate drought severity several months in advance. As long as instrumental series of the NAO and WI are available, their combined use would allow inferring European drought variability for the last two centuries and improve the calibration and interpretation of paleoclimatic proxies associated with drought.

Key-words: Climate variability, atmospheric circulation, evapotranspiration, Standardized Precipitation Evapotranspiration Index, NAO, SPEI, non-stationary, drought proxies, Westerly Index.

1. Introduction

Drought is one of the most important natural hazards affecting Europe. It causes noticeable environmental damages, including forest mortality (Carnicer et al., 2011), risk of forest fires (Pausas, 2004) and potential land degradation and desertification processes (Vicente-Serrano et al., 2012a). Moreover, economic losses associated with droughts have substantially increased in the past two decades, rising to EUR 6.2 billion yr^{-1} (EEA, 2010). For these reasons, the scientific research on droughts is a priority, and different pan-European

initiatives have been promoted to improve drought monitoring and early warning, such as the European Drought Observatory (<http://edo.jrc.ec.europa.eu/>; last accessed 5 November 2014) and drought forecasting products derived from the variable resolution ensemble prediction system of the European Centre for Medium range Weather Forecast (ECMWF) (Singleton, 2012).

Nevertheless, despite the efforts in developing physically-based drought forecasts, the skill of models is usually low, given the strong variability of European droughts and the complex climate forcing interactions at regional scales. For these reasons, a better understanding of the driving mechanisms of drought variability in Europe is crucial, since they may bring some improvement in monitoring and in the statistical forecasting of droughts (e.g., http://www.cpc.ncep.noaa.gov/products/expert_assessment/sdo_summary.html; last accessed 5 November 2014).

Atmospheric circulation is one of the key drivers of droughts. The atmospheric patterns associated with European droughts are complex though, mainly due to the different spatial scales involved, from the general atmospheric circulation (Van der Schrier et al., 2006), to synoptic weather types (Vicente-Serrano and López-Moreno, 2006). The North Atlantic Oscillation (NAO) is the main atmospheric circulation pattern in the North Atlantic sector, and affects the surface climate of large parts of Europe (Wanner et al., 2001; Trigo et al., 2002; Hurrell et al., 2003). Several studies have shown the strong influence of the NAO on drought variability across Europe (e.g., Van der Schrier et al., 2006; López-Moreno and Vicente-Serrano, 2008; Sousa et al., 2011), even suggesting some skill of this index on drought forecasting (e.g., Santos et al., 2014). However, the NAO impact on drought across Europe displays noticeable spatial differences, being strong in Southern Europe but weak in other European areas (Trigo et al., 2002). This stresses the need of exploring other atmospheric indices to explain drought variability across entire Europe and explore its stationarity. Studies have suggested the influence of other Northern Hemisphere atmospheric circulation patterns on European drought variability at the regional level. Among them, the most important ones are the East Atlantic Pattern (EA), the Scandinavian Pattern (SCAN) and the East Atlantic-West Russian Pattern (EA-WR) (Barnston and Livezey, 1987; Trigo and Palutikof, 2001). These indices influence the surface climate over large regions of Europe (e.g., Trigo and Palutikof, 2001; Trigo et al., 2008; Comas-Bru and

McDermott, 2013) and show a clear connection with drought variability (e.g., Sousa et al., 2011; Van der Schrier et al., 2006; Kingston et al., 2014; Ionita, 2014), thus suggesting that they could spatially complement the NAO signal in drought variability across the continent. A major shortcoming of these indices is the short period of data availability (roughly, from the mid 20th century), which restricts their use for long-term climate studies and the assessment of low-frequency (multidecadal) variability of droughts. On the contrary, monthly NAO time series from instrumental records extend back to the beginning of the 19th century (Jones et al., 1997). For this reason, investigations focusing on the long-term variability of droughts and precipitation in Europe have mainly used the NAO as the only indicator of the influence of atmospheric circulation on the European climate (e.g., Vicente-Serrano and López-Moreno, 2008a). In addition to instrumental-based NAO indices, there are also multi-proxy reconstructions of the NAO and other circulation indices based on long historical instrumental series and indirect indicators (e.g., tree-rings, ice cores, documentary sources, etc.), which allow extending its record beyond the 19th century (e.g., Luterbacher et al., 1999, 2002; Folland et al., 2009). However, these reconstructions often involve large uncertainties in the NAO estimations and important discrepancies among them (e.g., Schmutz et al., 2000). This stresses the importance of recovering historical instrumental data in order to provide a more accurate representation of the atmospheric mechanisms driving drought variability in Europe.

Barriopedro et al. (2014) have recently developed an atmospheric circulation index called the Westerly Index (WI), which measures the frequency of days with westerly winds over the English Channel. The advantage of the WI regarding the NAO is related to the availability of records back to the 17th century. The WI shows a robust signal on precipitation and temperature over large parts of Europe, and Barriopedro et al. (2014) found that the WI and the NAO are complementary in terms of their information on the atmospheric circulation over the Euro-Atlantic sector, and their associated impacts on temperature and precipitation.

In this study we have used a synthetic drought index (the Standardized Precipitation Evapotranspiration Index: SPEI), obtained on different time-scales, to analyse the impact of the WI on drought variability across Europe, and to compare it with the NAO signal and further circulation patterns that are relevant for the European climate (Clnet and Martin, 1992; Wibig, 1999; Qian et al., 2000).

105 Previous studies on this topic have only focused on precipitation data (Hurrell and Van Loon, 1997;
106 Zveryaev, 2006), precipitation-derived drought indices, like the Standardized Precipitation Index (SPI)
107 (López-Moreno and Vicente-Serrano, 2008) or other drought indices, such as the Palmer Drought Severity
108 Index (PDSI, Van der Schrier et al., 2006; Sousa et al., 2011), which do not consider multiple time-scales
109 that characterize droughts (McKee et al., 1993). As an important novelty, this study provides a step forward
110 in the body of knowledge on drought severity by using the SPEI, which accounts for two essential
111 components of droughts: (i) the atmospheric evaporative demand, which allows interpreting drought as an
112 imbalance between water availability and the water demand and (ii) different drought time-scales, which
113 characterize different drought types and impacts (e.g., Vicente-Serrano et al., 2013; Lorenzo-Lacruz et al.,
114 2013).

115 The spatio-temporal variability of droughts across Europe is pronounced (e.g., Lloyd-Hughes and
116 Saunders, 2002) and the time scale over which water deficits accumulate is crucial for the assessment of
117 drought impacts on different hydrological systems. In this sense, the SPEI has shown capacity to detect
118 different drought impacts on a suite of hydrological, agricultural and ecological variables at the global scale
119 (including Europe) better than drought indices only based on precipitation (Vicente-Serrano et al., 2012b).
120 The influence of the SPEI on these hydro-ecological systems occurs on different time-scales, since the
121 period from the arrival of water inputs to usable water resources differs among systems (McKee et al.,
122 1993). Soil moisture (Scaini et al., 2014), streamflow (Haslinger et al., 2014), reservoir storages (Lorenzo-
123 Lacruz et al., 2010), crop productions (Potop et al., 2012) and vegetation dynamics (Camarero et al., 2013;
124 Ivits et al., 2014) are among the variables correlated with SPEI and other drought indices. These variables
125 are influenced by the atmospheric circulation and the persistence of anomalous situations, which, in turn,
126 can be summarized in several circulation indices. This stresses the importance of assessing the relationships
127 between atmospheric circulation indices and the SPEI variability, since these relationships can be useful to
128 identify different drought-related impacts.

129 The objectives of this study are: (i) to assess the response of SPEI on different time-scales to various
130 indices that characterize atmospheric circulation variability over Europe for 1950-2008; (ii) to compare the
131 NAO and WI signals in the multi-scalar SPEI over a longer period (1900-2008); and (iii) to determine the

temporal stability and changes in the spatial pattern of these relationships over this period. We also explore the possible predictability of droughts in Europe by considering different lags among atmospheric circulation indices and drought time-scales, which could also open the opportunity for improving drought early warning across the continent.

2. Datasets and methods

2.1. Drought data

To determine drought severity across Europe, we have used the monthly SPEI (Vicente-Serrano et al., 2010a). The SPEI is especially well suited for studies analyzing the effect of global warming on drought severity. The SPEI considers the effect of reference evapotranspiration on drought severity and, different to the PDSI, enables identification of different drought types and impacts on diverse systems (Vicente-Serrano et al., 2012b, 2013). Vicente-Serrano et al. (2010a, 2010b, 2011a, 2012b, 2014) and Beguería et al. (2014) provided complete descriptions of the physical rationale behind the SPEI, the computational details, and comparisons with other widely-used drought indicators such as the PDSI (Palmer, 1965) and the SPI (McKee et al., 1993). The SPEI measures the “climatic water balance” as the difference between available water (i.e., precipitation, P) and the atmospheric water demand (or reference evapotranspiration, ET_o), and therefore provides a more reliable measure of drought severity than precipitation alone. The climatic water balance is calculated at various time scales (i.e. over 1-month, 2-months, 3-months, etc.), and the resulting values are fit to a log-logistic probability distribution to transform the original values to standardized units that are comparable in space and time and at different SPEI time scales. Negative SPEI values represent below-normal (dry) conditions and positive values represent above-normal (humid) conditions.

Some authors have criticized the SPEI in relation to the PDSI, arguing that the SPEI does not represent soil water content (Dai, 2011; Joetzjer, 2014). However, the SPEI represents departures from the climatological balance between water availability and atmospheric water demand, and it is therefore different from the PDSI, which rather estimates the soil moisture budget through a simplified model (Beguería et al., 2014). Moreover, the SPEI is not affected by problems of spatial comparability, as is the case of PDSI (Guttman, 1998; Vicente-Serrano et al., 2010b), and is perfectly comparable among sites and

time scales. In addition, the SPEI has showed better capacity than other drought indices to identify drought impacts in a variety of agricultural, hydrological and ecological systems at the global scale (Vicente-Serrano et al., 2012b).

The SPEI has been obtained from the global SPEI database (SPEIbase, Beguería et al., 2010) at the spatial resolution of 0.5° and the period 1902-2008 (<http://sac.csic.es/spei/database.html>; last accessed 5 November 2014). The SPEI is calculated from monthly precipitation and ETo data (TS3.20 version) of the Climatic Research Unit (CRU) of the University of East Anglia. ETo is based on the FAO-56 Penman-Monteith estimation (Allen et al., 1998), which is directly calculated by the CRU. To explore the multi-scalar character of drought variability, we have used the SPEI time series for 3-, 6-, 9- and 12-month time-scales.

2.2. Atmospheric circulation indices

The WI is defined as the proportion of days in a month with prevailing wind direction from the west quadrant over the English Channel (cf. [-10, 5]°E, [48,52]°N), and is the longest instrumental record of atmospheric circulation over the eastern Atlantic to date (1685-2008). It has been obtained from daily marine observations of wind direction only by using the Royal Navy ships' logbooks for the 1685-1850 period and the CLIWOC v1.5 and the ICOADs v2.1 datasets since 1851 (see Wheeler et al., 2010 and Barriopedro et al. 2014 for further details). In this study, we have used monthly time series of the WI for the period 1902-2008. Different to other zonal circulation indices such as the Paris-London index or Western Europe zonal index (Slonosky et al., 2000, Cornes et al 2012 Luterbacher et al. 1999), the WI is more sensitive to the direction of the true wind than to the strength of its geostrophic component. Overall the WI is more strongly related to precipitation anomalies mainly in northern Europe than the NAO or the Paris-London index (see Barriopedro et al 2014 for further discussion). An advantage of the WI is that the associated signal (mainly in precipitation) is robust through the year, and also that its record can be extended further back in time than that of the NAO or even the one of the Paris-London index (which has frequent missing data in the 17th century). In addition, and different to indices based on pressure data, the WI does not require correction or calibration. See Barriopedro et al (2014) for further discussion on this issue.

Different NAO indices are available in the literature. Monthly series of the NAO can be obtained as:
 (i) the pressure difference between two fixed stations located in the northern and southern North Atlantic area (NAOi, hereafter; e.g., Hurrell et al. 2003), or (ii) the leading mode of atmospheric circulation variability, as obtained from a Rotated Principal Component Analysis (RPCA) of either sea-level pressure (SLP) or geopotential height at 500 hPa (Z500) over the North Atlantic (NAO-PC, hereafter; e.g., Hurrell and Deser 2009). In the former definition, it is common to use observatories in Iceland (Reykjavik and Stykkisholmur) as the northern node, and either Lisbon (Hurrell, 1995) or Gibraltar (Jones et al., 1997) as the southern node. NAOi time series extend further back in time than NAO-PC indices, and hence they are preferred for long-term climate studies. However, different to NAO-PC indices, the NAOi does not account for the seasonal changes in the spatial pattern of the NAO. Several authors have concluded that station-based indices do not provide an optimal representation of the NAO (Wallace, 2000; Folland et al., 2009), mainly in the warm season (Blade et al., 2012; Pokorna and Huth 2014), because of the seasonal displacement of the Iceland low and the Azores anticyclone (Portis et al., 2001). Therefore, in this study we have employed both versions of the NAO. For 1902-2008, we used the NAOi developed by Jones et al. (1997), which is based on Gibraltar (southwest Iberian Peninsula) and Reykjavik (southwest Iceland) stations. The NAOi was provided by the CRU (<http://www.cru.uea.ac.uk/cru/data/nao.htm>; last accessed 5 November 2014). For 1950-2008, we have also used a monthly NAO-PC index, obtained from a Rotated Principal Component Analysis (RPCA) of three-month centered anomalies of Z500 (available at <http://www.cpc.ncep.noaa.gov/data/teledoc/telecontents.shtml>). The WI and NAO provide different approaches to characterize the zonal flow over the eastern Atlantic and they actually record distinctive aspects of the atmospheric circulation (Barriopedro et al. 2014); with the exception of winter, the percentage of the WI variance explained by the NAOi is low (Figure 1). For 1950-2008, we have also used other circulation monthly indices in order to establish comparisons with the results found for the WI and NAO. They have been obtained from the same RPCA that was employed to derive the NAO-PC (Barnston and Livezey, 1987), and they are available since 1950 at the NOAA website (<http://www.cpc.ncep.noaa.gov/data/teledoc/telecontents.shtml>). The indices selected for this study were the East Atlantic (EA), Scandinavian (SCAN) and East Atlantic-Western Russian (EA-WR). Trigo and

Palutikof (2001) showed that these patterns explain a high percentage of variance of the European atmospheric circulation in winter, spring and autumn. In addition, Sousa et al. (2011) found that the NAO and the SCAN patterns were the most important drivers of drought severity in the Mediterranean region. Table 1 shows the percentage of the variance of WI explained by these atmospheric circulation indices for 1950-2008. The seasonal and annual WI variability explained by the different indices obtained from PCA is very low. Only the NAO-PC explains more than 40% of the WI in winter, this confirms the fact that WI is independent from the other indices.

2.3. Methods

The series of the atmospheric circulation indices described in the last section were first expressed on the same time-scales as those used for the SPEI (i.e., 3-, 6-, 9- and 12-months) by simply averaging their monthly values over the current month and also the previous 2-, 5-, 8- and 11-months, respectively. Seasonal series of the circulation indices were derived for February (winter), May (spring), August (summer) and November (autumn). Spatial correlation maps were obtained by computing Pearson's correlation coefficients between the seasonal series of the SPEI and each circulation index (NAOi, WI, NAO-PC, EA, SCAN and EA-WR) for 1950-2008. Similarly, we calculated seasonal correlations between the SPEI and the NAOi and WI for 1902-2008. These seasonal correlations were computed separately for each of the four time-scales considered (i.e., 3-, 6-, 9- and 12-months), thus accounting for the “direct” influence of the circulation indices on drought variability on different time-scales. No significant serial correlation beyond lag-0 at the $p < 0.05$ was found. This was expected since the maximum SPEI time-scale used in this study was 12 months and the correlations were obtained annually. It means that the drought conditions of past years do not affect drought indices of the current year (as it happens considering longer drought time-scales, e.g. 24- or 36-month). This was taken into account when designing the experimental analysis and therefore no pre-whitening for removing any significant autocorrelation was applied.

In addition, the predictive skill of the circulation indices to determine drought variability was assessed by means of lagged correlations between the SPEI recorded in a given season and the atmospheric circulation

indices from the previous seasons. Thus, the 3-month winter SPEI was correlated with the 3-month winter circulation indices, which corresponds to a 0-month lag. The 6-month winter SPEI was correlated with the 3-month and 6-month winter indices (0 seasonal lag) and with the 3-month indices of the previous autumn (-1 seasonal lag). The 9-month winter SPEI was correlated with the 3-, 6- and 9-month winter indices (0 seasonal lag), with the 3- and 6-month autumn indices (-1 seasonal lag) and with the 3-month indices of the previous summer (-2 seasonal lag). Finally, the 12-month winter SPEI was correlated with the 3-, 6-, 9- and 12-month winter indices (0 seasonal lag), with the 3-, 6-, and 9-month autumn indices (seasonal lag), with the 3- and 6-month summer indices (-2 seasonal lag) and with the 3-month spring indices (-3 seasonal lag). The same approach has been followed with the other seasons. Significant correlations were set at the level of significance of $p < 0.05$.

To check whether the links found between the circulation indices and drought variability are robust in time we analyzed the temporal stability of the correlations patterns between the SPEI and NAOi and WI over the 1902-2008 period. This is motivated because several studies have reported a non-stationary influence of the atmospheric circulation on the European climate (e.g., Jung et al., 2003; Beranová and Huth, 2008; Vicente-Serrano and López-Moreno, 2008a; Barriopedro et al. 2014), and this could also be the case for the NAOi and WI influence on drought severity across Europe. To account for non-stationary effects, we have computed 31-year moving window correlations between the SPEI and each circulation index. The analysis has been applied to: (i) short-term (3-month) winter drought variability, since winter is the season in which atmospheric circulation is more important to explain the climate variability in Europe; and (ii) long-term (9-month) summer drought variability, which is relevant given the natural summer dryness in Europe and common reduction in the available water resources. Note that the 9-month time-scale chosen for summer drought is often the result of accumulated water deficits during the rainy seasons which determine water uses in the summer season (irrigation, urban supply, etc). On the contrary, water availability and water use in winter are not so dependent on precedent climate conditions.

In addition, to identify the spatial patterns of variability affecting the stationary influence of NAOi and WI on drought, we applied a S-mode PCA, in which the input variables were the time-series of 31-year moving window correlations between the short-term (long-term) winter (summer) SPEI and the circulation

index. In other words, the time series of moving correlations from individual grid-points form the columns of the input matrix for the PCA, which synthesizes in a small number of new uncorrelated variables a large fraction of the total variation in the analyzed time series. This procedure has been widely applied in climatological studies (see Richman, 1986; Jolliffe, 1986; Huth, 2006). A correlation matrix was selected to provide an efficient representation of variance within the data set in the PCA (Barry and Carleton, 2001). We retained the components (spatial patterns) that accumulated at least the 80% of the total variance. The associated time series were represented by the original units (i.e., Pearson's correlation coefficients).

274

275 **3. Results**

276 *3.1. Influence of different atmospheric circulation indices on SPEI variability*

277 The top rows of panels in Figure 2 show the seasonal correlation maps between the 3-month SPEI and the concurrent seasonal series of the circulation indices NAOi, WI, NAO-PC, EA, SCAN and EA-WR. Therefore, they summarize the “immediate” seasonal responses in short-term drought severity to the atmospheric circulation features represented by each index. The drought severity response shows large differences across Europe and among seasons. In winter, drought variability is well explained by a small number of atmospheric circulation patterns. Thus, the NAOi clearly determines the winter drought variability in southern (negative correlations) and northern (positive correlations) Europe, as a consequence of its control of precipitation in comparison to ETo (Figures 3 and 4). In southern (northern) Europe droughts are favored by positive (negative) NAOi. There are not important differences between the NAOi and the NAO-PC. The WI pattern is similar to the NAO, but it also correlates with SPEI over large regions of central Europe. It means that high WI values correspond to humid conditions in North Europe and dry in South Europe, with the influence limited to regions smaller than the NAO in southern parts of Europe. The EA pattern shows weaker responses in SPEI, except in the British Islands and some areas of Scandinavia, France and the Iberian Peninsula. SCAN shows an opposite pattern to that of the NAO and WI, but with much weaker (and positive) correlations in southern Europe and stronger (and negative) signals in Russia. They result from the blocking pattern over Scandinavia associated with the positive phase of this mode, and its effect in the storm tracks and precipitation anomalies, favoring drought conditions across this region.

294 This positive phase of SCAN is also characterized by low pressures over western Europe, which explains
 295 that positive values of this circulation index favor humid conditions in Iberia and the Mediterranean region,
 296 also favored by a negative influence on ETo (Figure 3). Thus, the SCAN modulates drought variability over
 297 large areas of northern Europe and the Mediterranean area. However, these regions also show significant
 298 (and even stronger) correlations with NAOi or WI. Similarly, and with the exception of France, the EA-WR
 299 pattern affects European regions that are also influenced by the NAOi or WI (e.g., southern Europe and the
 300 Balkans). The blocking pattern over central Europe associated with the positive EA-WR phase favors
 301 drought conditions in this region, and explains the negative correlation between SPEI and EA-WR over
 302 large areas of central Europe.

303 In spring the influence of the circulation indices on drought variability decreases in both magnitude and
 304 spatial extension. This is particularly acute for the NAO (both NAOi and NAO-PC) and EA-WR, whereas
 305 the influence of WI and SCAN is similar to that in winter, with significant SPEI responses over large areas
 306 of central and southern Europe and Scandinavia, respectively.

307 In summer there are strong differences between the correlation patterns of the NAOi and the NAO-PC, with
 308 the former showing weak signals in SPEI, and the latter displaying similar (but opposite in sign) responses
 309 to those obtained for the WI. The differences between NAOi and NAO-PC are due to the seasonal changes
 310 in the centers of variability, which in summer are placed over the UK and Greenland, as captured by the
 311 NAO-PC, but not by the station-based NAOi. The summer WI exerts a strong influence on drought
 312 variability over large areas of central and northern Europe, driven by its control on precipitation (Figure 4),
 313 while its influence over southern Europe weakens (as compared to winter and spring), being restricted to the
 314 Balkans. Although the correlation between summer WI and NAO-PC is not strong (Pearson's $r = -0.45$), the
 315 similarity of the WI and NAO-PC responses indicates that positive phases of the summer WI are associated
 316 with low pressures over the UK, thus resembling negative phases of the summer NAO. Summer short-scale
 317 droughts in southern Europe are better explained by EA and SCAN, than by NAOi or WI. This is due to the
 318 location of a high pressure centre in southern Europe and the Mediterranean area corresponding to the EA,
 319 and a low pressure centered over the Iberian Peninsula for SCAN. These atmospheric configurations cause
 320 that summer positive (negative) EA (SCAN) conditions may favor droughts in southern Europe. In these

areas, temperature is expected to play an important role in SPEI by modulating the atmospheric water demand. Thus, the EA and SCAN signals in SPEI result from the combined effect of enhancing atmospheric water demand and precipitation deficits, which both contribute to enhance drought occurrence (Figures 3 and 4). Note, however, that short-term summer droughts are not very meaningful in some Mediterranean regions due to the lack of summer precipitation. SCAN and EA-WR also show significant correlations with drought variability in northern Europe also by a combination of the influence on ETo and precipitation, but most of these regions are also influenced by the WI.

In autumn there are still discrepancies in the drought responses to NAOi and NAO-PC. The NAOi pattern resembles that of the winter in southern Europe, but not in northern Europe, where its influence is negligible. On the contrary, the NAO-PC shows a clearer pattern, which is shifted to the south, as compared to that of summer. Different to the other circulation indices, the WI and SCAN show similar responses to those obtained in the other seasons, which means a high intra-seasonal stability in their influence on the SPEI.

The bottom row of Figure 2 shows the correlations between summer long-term drought (represented here by the summer 9-month SPEI) and the corresponding 9-month circulation indices, thus representing the accumulated effect of the atmospheric circulation on long-term drought. Overall, the SPEI responses resemble the average of the seasonal correlation patterns described above. Due to the seasonal-changing patterns of the NAO-PC, the magnitude and spatial extent of significant correlations between the NAOi and the SPEI are stronger and more consistent than those for the NAO-PC. The NAOi influence in long-term southern Europe drought severity is also higher than that found with any other index. Moreover, and with the exception of easternmost Europe, the regions that do not show significant correlations with the NAOi are significantly correlated with WI (British Islands, North France, Denmark, Low Countries, North Germany and large areas of Scandinavia). This suggests that the WI complements the NAOi signal in long-term summer droughts in Europe, and that the combined use of these indices is able to better explain drought variability than any other indices across Europe.

Figure 5 shows Pearson's correlation coefficients between circulation indices and different SPEI time-scales over six representative regions. In the North of the British islands (region 1) the WI shows high correlations (Pearson's $r > 0.5$) in the different seasons and time scales. It controls short-term droughts (3-month SPEI)

but it also shows drought predictive capacity some months in advance. For example, 9-month summer SPEI shows correlation with 3-month winter WI. The propagation of the short-term signal of atmospheric circulation patterns on long time-scale drought (e.g., 9- and 12-month) in the different regions is mainly explained by the relative importance of precipitation or reference evapotranspiration of each season regarding the total annual. In the region 1, the WI clearly improves the predictive skill of SPEI by NAOi and EA. In Southern Scandinavia (region 2), and Low Countries and North Germany (region 3), the WI correlates better with SPEI than the other circulation indices. In South France (region4), the SCAN shows best skill for drought prediction in spring, and the NAOi shows few differences with SCAN in summer. In Southern Europe the SPEI correlates with different circulation indices. In Iberia (region 5), the SPEI correlates with NAOi, WI, NAO-PC and SCAN, although strongest correlations are obtained with NAOi. In the Balkans (region 6), drought variability is controlled by NAOi. Here NAOi and NAO-PC show similar correlations in the four seasons and different SPEI time-scales. The few significant correlations found between some long-term averaged modes obtained from PCA (NAO-PC and EA-WR) and long SPEI time-scales measured in the different regions is probably related to the changes in the intra-annual position of the action centres that characterizes these modes. This limits their use for long-term droughts, since they do not reflect any circulation pattern common for the long periods. Nevertheless, other atmospheric circulation patterns also obtained from PCA, which show few seasonal changes in the spatial configuration of the action centres (e.g., SCA), show strong correlation with SPEI long-time scales.

Although some of the circulation indices show high correlations with the SPEI in different regions and seasons of the year (e.g., SCAN), the NAOi and WI show complementary signals in SPEI across most of Europe and for all seasons and different time-scales. Note also that the NAO-PC does not add much to the explanatory capacity of drought encountered by the NAOi and WI in winter and summer. Thus, although the NAO-PC explains short-term summer drought severity better than the NAOi, its pattern is well captured by the WI. Consequently, from now on, we will focus on the analysis of the NAOi and WI alone. For simplicity, in the remaining of this section the station-based NAOi index will be referred to as NAO.

Another important advantage of the NAO and WI indices is the longer periods for which they are available. It allows establishing more robust linkages between atmospheric circulation and drought variability than

375 those found in the previous section, and address the stability of their relationships throughout the period of
 376 data availability. Considering the 1902-2008 period for the NAO and WI, we find similar patterns to those
 377 found in the short period, with positive phases of the WI leading to humid conditions over an area
 378 embracing UK, Scandinavia and most western Europe (Fig. 6). This pattern exhibits low seasonal
 379 variability. The correlation is negative in most of southern Europe, but displays an erratic behavior through
 380 the year, with stronger WI signals in winter and autumn. During these seasons, the NAO pattern in southern
 381 Europe is stronger and extends over larger areas than that of WI. The NAO also shows significant positive
 382 correlations over northern Europe, but, different to the WI, they are limited to winter. The influence of WI
 383 and NAO on winter drought is similar, since in this season both indices capture similar aspects of the
 384 atmospheric circulation (Fig. 1). However, in the transitional seasons, and more prominently in summer,
 385 their signals in drought severity are very different, as are their circulation patterns, with the summer WI
 386 being related to regional anomalous atmospheric conditions centered over the UK, rather than changes in the
 387 large-scale pressure gradient between Iceland and Azores (Barriopedro et al., 2014).
 388 The long-term droughts patterns during the dry season are also similar to those of the short period, with a
 389 NAO signal in southern Europe, France, eastern UK and some regions of Scandinavia. The winter-to-
 390 summer mean of the WI shows strong positive correlations with long-term summer droughts in most of
 391 Scandinavia, the British islands and large areas of central and eastern Europe. Again, Fig. 4 confirms the
 392 results obtained for the second half of the 20th century. These results suggest that drought should be more
 393 predictable from WI in northern Europe, and from NAO in southern Europe. In summary, the NAO is a
 394 good indicator of short-term droughts in southern Europe for winter and autumn, while the WI captures
 395 better the variability of northern European droughts throughout the whole year. Moreover, WI also shows
 396 some predictive capacity of droughts in central Europe seasonally but also for the summer long-term
 397 droughts, since significant correlations between WI and the SPEI have been found in Germany, Switzerland
 398 and even regions of Poland and the Czech Republic. The NAO also complements WI in other regions of
 399 Eastern Europe, its influence reaching the Black Sea region in winter and autumn. This stresses that the
 400 complementary role of NAO and WI in explaining drought variability across large regions of Europe is
 401 observed for the entire 20th century and hence that the combined influence of these “pairwise modes” is a

robust signature of the atmospheric circulation. This is confirmed by means of the pattern relationship between the NAO and WI correlations with SPEI. Figure 7 shows the relationship between the spatial correlation patterns for the different seasons and the summer long-term drought. In winter the relationship is high, although in areas with negative values (corresponding to Southern Europe) the magnitude of the correlation is higher for the NAO than for the WI and the opposite is found in areas with positive correlations (Northern Europe). For spring, summer and autumn and for the summer long-term droughts the spatial correlation patterns between the SPEI and WI and NAO are very different. This stresses the fact that these two atmospheric circulation indices differentially affect drought variability in Europe and they are complementary both spatially and seasonally.

3.2. Non-stationary relationships

We now explore whether the NAO and WI signals on drought severity are stationary over the entire 1902-2008 period. Figure 8 shows the correlation of the NAO and WI with the winter short-term and the summer long-term SPEI for three consecutive 31-year periods: 1916-1946, 1947-1977 and 1978-2008 (similar results were found for other seasons and temporal scales, not shown). The results show that there are noticeable temporal variations in the responses of European droughts to the NAO and WI, but the spatial patterns of correlations show important similarities for the three analyzed periods. In winter, the NAO influence on the SPEI in southern Europe was more important prior to 1978, although there are not large differences between sub-periods in the magnitude of correlations over the Iberian Peninsula, Italy and the Balkans. The differences in northern Europe are more relevant, as they indicate a strong NAO influence on short-term droughts over Scandinavia and other regions of northern Europe for 1978-2008, but weak NAO effects before 1978. Nevertheless, the WI-SPEI relationships in northern Europe are more stationary than those obtained for the NAO. It seems that the impact of the WI on short-term winter droughts has also become stronger through the 20th century over large parts of southern Europe, mainly over Iberia, where the strength of the WI signal is similar to that found for the NAO. Results for the long-term summer droughts show small differences among periods, but they also suggest that the WI pattern is more stationary in northern Europe than is the NAO pattern in southern Europe.

Figure 9 shows the spatial patterns responsible for the non-stationary component of the drought-circulation links according to the PCA analysis based on the 31-year moving window correlation series between each circulation index and SPEI. The first PCs (PC1) of the winter correlation series of the short-term SPEI with the NAO and WI account for the largest percentage of variance in the moving window correlation series (47% and 45% for the NAO and WI, respectively) and show an increase since the 1950s (Figure 9A). The associated spatial patterns (EOF1) show a clear southwest-northeast gradient for both indices (Figure 9B). Note that the EOF1s resemble the climatological spatial correlation patterns of Figure 6 and hence anomalous values of the corresponding PC1s denote a strengthening or weakening of this pattern. As PC1s indicate a positive trend since the 1950s, it means that the correlations between the winter SPEI and the winter NAO and WI have reinforced, with the last decades showing more negative relationships in southern Europe, and more positive relationships in northern and eastern Europe. In particular, the strengthened influence of the WI on winter drought variability has been more important over Iberia and France.

The rest of the components represent lower percentages of the variance but some of them show clear spatial patterns. PC2 for the winter NAO shows a change from negligible values at the beginning of the 20th century to strong negative values in the 1940s and relatively smaller importance thereafter. Its spatial pattern is associated with more positive NAO correlations in the mid latitudes of western Europe and the Balkans, where the climatological influence of the NAO shows meridional gradients (i.e., a transition from negative to positive correlations) and negative correlations, respectively (Fig. 6). Thus, the prevailing negative values of PC2 in the mid of the 20th century are indicative of strengthening of the winter NAO influence on the Balkans and a northward shift of the zero correlation line in western Europe. Similarly, PC3 for the winter WI shows stronger winter WI-SPEI correlations since 1980, affecting mainly to central France and the Low Countries.

PC1 of the long-term summer correlations between the NAO and the SPEI displays a trend towards negative values through the 20th century, which means a reinforcement of the negative correlations in southern Europe and of the positive correlations in northern Scandinavia, similar to the PC1 of the short-term winter correlations, but also a weakening (and even a reversal of the correlation signs) in central and

western Europe. The observed changes in the long-term summer WI-SPEI relationship are more complex. In Iberia and France there was a reinforcement of the WI influence (PC1) between 1950 and 1980. In central Europe and the Balkans the first period (1902-1950) was characterized by an increase of the WI influence (negative correlation) but since 1950s it has returned to near normal values.

Finally, it should be stressed that, despite the lack of stationarity in the SPEI responses to the circulation indices, the magnitude of the PCs is often below 0.4 (Fig. 9A), which implies relatively small changes in the correlation coefficients over many European areas (Fig. 9B), as compared to those obtained for the entire 1902-2008 period in regions of northern (> 0.7) and southern Europe (< -0.7). Therefore, the results found herein reinforce the main conclusion of section 3.1, i.e., that the NAO and WI effects on European drought severity are robust over large regions of Europe through the 20th century on different seasons and time-scales, and that their combined information is able to explain (and provide some predictive skill of) drought variability across Europe.

4. Discussion and conclusions

Several studies have shown that different atmospheric circulation patterns may play a role in explaining European drought variability. For example, Van der Schrier et al. (2006) found that the summer PDSI is correlated with winter NAO and EA patterns in different regions of Europe. Kingston et al. (2014) used 6-month SPEI data to stress the influence of the EA-WR pattern on drought severity over western and central Europe in spring, as a consequence of the weaker maritime influence during the positive phase of this pattern. Using 3-month SPEI data, Ionita (2014) reported that the winter EA-WR pattern also explains drought variability of large regions of central Europe and the Balkans, and shows some predictive capacity for spring drought conditions. On the other hand, Sousa et al. (2011) found a major influence of NAO and SCAN on PDSI variability over the Mediterranean region, with winter values of these circulation indices being correlated with PDSI values of the same and the following seasons. On the contrary, they stressed that EA-WR and EA patterns do not have robust influence on Mediterranean drought conditions. The results obtained in our study mostly agree with these previous assessments of the atmospheric circulation impacts on drought severity across Europe. Nevertheless, by including different SPEI time-scales and seasonal lags,

we have found that the signal of the EA and EA-WR patterns on drought is weaker than that obtained with other circulation indices (e.g., NAO and SCAN). This is because correlations of the SPEI with EA and EA-WR show strong seasonal differences in magnitude and the spatial patterns, and with the exception of the winter EA-WR, they do not show a large control of droughts in Europe, when compared to the other indices. On the contrary, the SCAN pattern shows strong seasonal stability in modulating short-term (3-month SPEI) and long-term (9-month SPEI) droughts over north-eastern and southern Europe.

The influence on the NAO on drought severity across Europe has been confirmed by different studies and drought indices (e.g., Van der Schrier et al., 2006; López-Moreno and Vicente-Serrano, 2008a; Sousa et al., 2011). Using the SPEI, we have shown that drought variability in large regions of Europe is clearly controlled by the NAO. Vicente-Serrano et al. (2011b) also showed that the NAO exerts a strong control on SPEI variability over southern Europe and some regions of North Africa. Nevertheless, here we have reported that the NAO influence on northern Europe drought variability is small, and limited to winter. Although lagged relationships between aggregated drought time-scales and the NAO show some predictive skill of the NAO to determine drought conditions in regions of southern Europe, the same ability is not observed in northern Europe, where NAO influence is restricted to few areas.

The poor performance of the NAO to explain drought variability in northern Europe partially depends on the choice of the NAO index. As stated above, the pressure centers that characterize the NAO experience a natural seasonal displacement. For this reason, the NAO index based on two fixed stations (here the Reykjavic-Gibraltar NAOi) could not represent the dominant mode of variability in summer and in transient seasons (Folland et al., 2009; Blade et al., 2012). We have shown that using a PC-based NAO index that accounts for the seasonal displacement of pressure centers (NAO-PC), the NAO influence on short-term (3-month SPEI) drought variability enhances over northern Europe (mainly during the warm season), but decreases over southern Europe (mainly in transient seasons), as compared to the station-based NAOi. The same result is observed for long-term droughts (summer 9-month SPEI). The reason of the weaker NAO-PC influence on long-term droughts is related to the definition of the index itself, since positive phases of the NAO-PC mean enhanced westerly flows over western Europe in winter, but anticyclonic conditions over the same region during summer. On the contrary, and despite its weaker signals in the warm season, the

NAOi shows stronger responses in long-term drought severity than the NAO-PC, since it represents a spatially coherent atmospheric configuration through the year, namely, the intensity of the zonal flow over the eastern North Atlantic.

From the above discussion, it follows that the NAOi and the SCAN pattern could be used to explain most of the drought variability across Europe at the short (seasonal) and long-term time-scales. However, based on the results of this study, we recommend using the WI instead of the SCAN pattern. Several arguments support this conclusion: (i) similar to SCAN, the WI influence on drought severity is seasonally stable (both spatially and in the magnitude of correlations) and hence is not affected by changes in the correlation pattern with the short-term SPEI (as it was observed with the NAO-PC); (ii) different to SCAN (or to NAOi), the WI accounts for much of the atmospheric signatures associated with the dominant mode of variability in the summer season. In fact, the magnitude and the spatial signatures of the WI signal on short-term summer drought are similar to those obtained with the summer NAO-PC; (iii) except for eastern Europe, the WI is able to explain seasonal short-term drought variability over northern Europe (including Scandinavia), as does the SCAN, but it also influences drought severity over large areas of central and western Europe, for which SCAN shows non-significant signals; (iv) the WI signal complements the spatial NAOi signatures in drought better than does the SCAN. In particular, both SCAN and NAOi lead to significant responses in southern Europe, and this “redundant” information affects long-term droughts and short-term seasonal droughts of most of the year. On the contrary, the WI and NAOi provide complementary spatial information of short-term and long-term droughts, except during the winter season; and (v) finally, the WI is available since the 17th century, which makes this index more useful than SCAN to explore droughts and their low-frequency variability in a long temporal context, as explained below. In summary, the variability of short-term seasonal drought severity over northern Europe and most of the British Islands is better explained by the WI than by other atmospheric circulation indices. In what concerns longer SPEI time-scales, which are relevant to assess drought severity in a variety of hydrological systems (e.g., López-Moreno et al., 2013), the WI also provides good predictability of long-term drought conditions over large regions of northern and central Europe. This is highly relevant, given the strong influence of evapotranspiration processes on determining long-term summer drought severity (Ciais et al., 2005).

On the other hand, our results indicate that the NAOi and WI together are able to explain drought severity across most of Europe. The more stable seasonal behavior of the WI in comparison to the NAOi could be explained by the different nature of these two atmospheric circulation indices. The NAOi is obtained from the pressure gradient between two stations that are situated in the centre of main pressure centres of the North Atlantic region, which are not geographically stable and show seasonal displacements. This affects the magnitude and direction of associated large-scale flows (Portis et al., 2001), and the sources of moisture fluxes into the European continent. On the contrary, the WI is based on the frequency of westerly flows in a single site (i.e., the English Channel), which enhances stable relationships between seasons. Therefore, the different patterns of correlations between the NAOi and WI and the SPEI across Europe suggest their spatial complementarity in terms of determining drought variability across the entire continent.

Overall, the spatial responses in drought to NAOi and WI resemble their respective signals in precipitation, which show a north-south dipole, with enhanced precipitation to the north and reduced precipitation to the south (e.g., Trigo et al. 2002; Barriopedro et al. 2014). These rainfall responses are in turn associated with the respective atmospheric circulation patterns, which modulate the storm tracks entering the continent. As expected, this suggests that the SPEI responses to atmospheric circulation are largely controlled by precipitation anomalies. This conclusion is supported by the following results: (i) for both NAO and WI, the signatures in drought severity resemble those in precipitation; (ii) similar to the seasonal SPEI patterns, the precipitation responses to WI are similar through the whole year, while the WI signals in temperature vary with season, showing cold temperatures in UK during summer, and warm temperatures in northern and central Europe during the rest of the year. Thus, an increased frequency of westerlies (positive WI) leads to enhanced precipitation and humid SPEI conditions over the UK, despite the occurrence of cold temperature.

The lagged correlations between the SPEI and NAOi and WI also suggest some skill of these indices to determine drought severity in different systems some months ahead. This capacity could be further improved from current physical models trying to predict European atmospheric circulation (Kushnir et al., 2006) and statistical models based on sea surface temperature and other variables (Santos et al., 2014).

Moreover, the results obtained from moving window correlations between the NAOi and WI and the SPEI have indicated that drought predictability based on these indices has increased over southern and northern Europe during the last decades. Although the predictive skill should be considered carefully given the relative level of non-stationarity shown in Fig. 6, some studies have suggested that under increased greenhouse gas emissions the stability of the NAO-climate correlations may be enhanced due to the lower variability in the spatial pattern of the NAO dipole (Vicente-Serrano and López-Moreno, 2008b). This would involve more predictable drought periods in southern Europe for this century. Further research is required to model the WI variability and its response to future climate change scenarios.

Our results have also implications from a paleoclimatic perspective. The availability of long instrumental series for the WI (since 1685, Barriopedro et al., 2014) and NAOi (from 1821, Jones et al., 1997) and their complementary role in droughts, make possible to infer both short-term and long-term drought variability in northern, southern and large areas of western and central Europe for the last centuries. The added value of the WI to improve drought reconstructions for long periods comes from the following facts: (i) the WI has a significant signal in drought severity through the year; (ii) many climate proxies are sensitive to drought for specific seasons of the year; (iii) the WI is the longest available instrumental-based record of atmospheric circulation, thus providing long targeting periods for proxy calibration; and (iv) the WI is a better index to calibrate drought/precipitation proxies of northern Europe than the NAO. Therefore, a reassessment of proxies including the WI information could refine our picture of drought variability in the last centuries (back to 1685), particularly over northern Europe. This information could be complemented with that of the NAO to provide a more detailed description of drought variability across Europe during the instrumental period.

We note in closing that different studies have provided multi-proxy European reconstructions of temperature and precipitation (e.g., Luterbacher et al. 2004; Pauling et al., 2006; Casty et al., 2007), from which droughts could be inferred, and there are also summer drought estimates since 1750 for central Europe using long instrumental series from sparse terrestrial sites (Briffa et al., 2009). Given the scarcity of historical records and the uncertainties of multi-proxy reconstructions (e.g., Jones et al., 2009), any instrumental observation would largely benefit current drought estimates of the last centuries. More specifically, current studies often

lack data from the ocean, mainly before 1850, and hence they miss key atmospheric circulation features over the North Atlantic, which are the main driver of the European climate, including drought variability. Accounting for instrumental marine observations, as those provided by ships' logbooks, has shown to largely improve current reconstructions (e.g., Küttel et al. 2010). Therefore, the WI provides direct knowledge on the atmospheric circulation of the last three centuries that can be used to improve current European reconstructions and to explore drought variability on very long (multidecadal) time-scales.

Acknowledgements

The authors wish to acknowledge Ricardo Trigo and one anonymous reviewer for their detailed and helpful comments to the original manuscript. The data for this paper are available at Spanish National Research Council repository (<http://sac.csic.es/spei/database.html>), at Climate Research Unit (<http://www.cru.uea.ac.uk/cru/data/nao/>) and the Climate Prediction centre of the NOAA (<http://www.cpc.ncep.noaa.gov/data/teledoc/telecontents.shtml>). This work was supported by the research project CGL2014-52135-C3-1-R and Red de variabilidad y cambio climático RECLIM (CGL2014-517221-REDT) financed by the Spanish Commission of Science and Technology and FEDER, Ephyslab (UVIGO-CSIC Associated Unit) and “LIFE12 ENV/ES/000536-Demonstration and validation of innovative methodology for regional climate change adaptation in the Mediterranean area (LIFE MEDACC)” financed by the LIFE programme. C. A-M received a postdoctoral fellowship # JCI-2011-10263. Iberdrola Renovable provided partial support from contracts.

References

- Allen RG, Pereira LS, Raes D, Smith M (1998) Crop evapotranspiration - Guidelines for computing crop water requirements - FAO Irrigation and drainage paper 56.
- Barnston AG, Livezey RE (1987) Classification, seasonality and persistence of low-frequency atmospheric circulation patterns. *Monthly Weather Review* 115: 1083-1126.

Barriopedro D, Gallego D, Álvarez-Castro MC, García-Herrera R., Wheeler D, Peña-Ortiz C, Barbosa SM
(2014) Witnessing North Atlantic westerlies variability from ships' logbooks (1685–2008). *Clim. Dyn.* 43: 939-955.

Beguiría S, Vicente-Serrano SM, Angulo M (2010) A multi-scalar global drought data set: the SPEIbase: A new gridded product for the analysis of drought variability and impacts. *Bulletin of the American Meteorological Society* 91: 1351-1354.

Beguiría S, Vicente-Serrano SM, Reig F, Latorre B (2014) Standardized Precipitation Evapotranspiration Index (SPEI) revisited: parameter fitting, evapotranspiration models, kernel weighting, tools, datasets and drought monitoring. *International Journal of Climatology* 34: 3001–3023.

Beranová R, Huth R (2008) Time variations of the effects of circulation variability modes on European temperature and precipitation in winter. *Int. J. Climatol* 28: 139–158.

Blade I, Liebmann B, Fortuny D, van Oldenborgh GJ (2001) Observed and simulated impacts of the summer NAO in Europe: implications for projected drying in the Mediterranean region. *Clim Dyn.* 39: 709-727.

Briffa KR, van der Schrier G, Jones P (2009) Wet and dry summers in Europe since 1750: evidence of increasing drought. *Int J Climatol* 29:1894–1905.

Camarero JJ, Manzanedo RD, Sanchez-Salguero R, Navarro-Cerrillo RM (2013) Growth response to climate and drought change along an aridity gradient in the southernmost *Pinus nigra* relict forests. *Annals of Forest Science* 70: 769-780.

Carnicer J et al. (2011) Widespread crown condition decline, food web disruption, and amplified tree mortality with increased climate change-type drought. *Proceedings of the National Academy of Sciences of the United States of America* 108: 1474-1478.

Casty C, Raible CC, Stocker TF, Wanner H, Luterbacher J (2007) A European pattern climatology 1766-2000. *Climate Dynamics* 29:791–805

Ciais Ph et al. (2005) Europe-wide reduction in primary productivity caused by the heat and drought in 2003. *Nature* 437:529–533.

642 Clinet S, Martin S (1992) 700-hPa geopotential height anomalies from a statistical analysis of the French
643 hemis data set. *Int. J. Climatol.* 12: 229-256

644 Comas-Bru L, McDermott F (2014) Impacts of the EA and SCA patterns on the European twentieth century
645 NAO–winter climate relationship. *Q.J.R. Meteorol. Soc.* 140: 354–363.

646 Cornes RC, Jones PD, Briffa KR, Osborn TJ (2012) Estimates of the North Atlantic Oscillation back to 1692
647 using a Paris–London westerly index. *Int J Climatol.* doi:10.1002/joc.3416

648 Dai A (2011) Characteristics and trends in various forms of the Palmer drought severity index during 1900–
649 2008. *J. Geophys. Res.* 116: D12115, DOI: 10.1029/2010JD015541.

650 EEA (2010) Mapping the impacts of natural hazards and technological accidents in Europe – An overview
651 of the last decade. EEA Technical Report, 144 pp., 13/2010, European Environment Agency,
652 Copenhagen, Denmark, doi:10.2800/62638, ISSN 1725-2237, 2010.

653 Folland CK, Knight J, Linderholm HW, Fereday D, Ineson S, Hurrell JW (2009) The Summer North
654 Atlantic Oscillation: Past, present, and future. *J Climate* 22: 1082-1103.

655 Guttman NB (1998) Comparing the Palmer Drought Index and the Standardized Precipitation Index. *J. Am.*
656 *Water Resour. Assoc.* 34: 113–121.

657 Haslinger K, Koffler D, Schöner W, Laaha G (2014) Exploring the link between meteorological drought and
658 streamflow: Effects of climate-catchment interaction, *Water Resour. Res.* 50:
659 doi:10.1002/2013WR015051.

660 Hurrell J (1995) Decadal trends in the North-Atlantic Oscillation: Regional temperatures and precipitation,
661 *Science* 269: 676– 679.

662 Hurrell J, van Loon H (1997) Decadal variations in climate associated with the North Atlantic Oscillation,
663 *Clim. Change* 36: 301– 336.

664 Hurrell J, Deser C (2009) North Atlantic climate variability: the role of the North Atlantic Oscillation. *J Mar*
665 *Syst* 78:28–41.

666 Hurrell J, Kushnir Y, Ottersen G, Visbeck M (2003) The North Atlantic Oscillation: Climate Significance
667 and Environmental Impacts, *Geophys. Monogr. Ser.*, vol. 134, 279 pp., AGU, Washington, D. C.

668 Huth R (2006) The effect of various methodological options on the detection of leading modes of sea level
669 pressure variability, *Tellus, Ser. A* 58: 121–130.

670 Ionita M (2014) The Impact of the East Atlantic/Western Russia Pattern on the Hydroclimatology of Europe
671 from Mid-Winter to Late Spring. *Climate* 2: 296-309.

672 Ivits E, Horion S, Fensholt R, Cherlet M (2014) Drought footprint on European ecosystems between 1999
673 and 2010 assessed by remotely sensed vegetation phenology and productivity. *Global Change*
674 *Biology* 20: 581-593.

675 Joetzjer E, Douville H, Delire C, Ciais P, Decharme B, Tyteca S (2013) Hydrologic benchmarking of
676 meteorological drought indices at interannual to climate change timescales: a case study over the
677 Amazon and Mississippi river basins. *Hydrol. Earth Syst. Sci.* 17: 4885-4895.

678 Jolliffe IT (1986) *Principal Component Analysis*, 271 pp., Springer, New York.

679 Jones PD, Jónsson T, Wheeler D (1997) Extension to the North Atlantic Oscillation using early instrumental
680 pressure observations from Gibraltar and south-west Iceland, *Int. J. Climatol.* 17: 1433 – 1450.

681 Jones PD et al. (2009) High-resolution palaeoclimatology of the last millennium: A review of current status
682 and future prospects. *Holocene* 19: 3-49.

683 Jung T et al. (2003), Characteristics of the recent eastward shift of interannual NAO variability, *J. Clim.*, 16,
684 3371– 3382.

685 Kingston D, Stagge J, Tallaksen L, Hannah, D (2014) European-scale drought: understanding connections
686 between atmospheric circulation and meteorological drought indices. *J. Climate*. doi:10.1175/JCLI-
687 D-14-00001.1, in press.

688 Kushnir Y, Robinson WA, Chang P, Robertson AW (2006) The physical basis for predicting Atlantic sector
689 seasonal-to-interannual climate variability. *Journal of Climate* 19: 5949-5970.

690 Küttel M, Xoplaki E, Gallego D, Luterbacher J, García-Herrera R, Allan R, Barriendos M, Jones PD,
691 Wheeler D, Wanner H (2010) The importance of ship log data: reconstructing North Atlantic,
692 European and Mediterranean sea level pressure fields back to 1750. *Clim Dyn* 34:1115–1128.

693 Lloyd-Hughes B, Saunders MA (2002): A drought climatology for Europe. *International Journal of*
694 *Climatology* 22: 1571-1592.

695 López-Moreno JI, Vicente-Serrano SM (2008) Extreme phases of the wintertime North Atlantic Oscillation
696 and drought occurrence over Europe: a multi-temporal-scale approach. *Journal of Climate* 21: 1220-
697 1243.

698 López-Moreno JI et al. (2013) Hydrological response to climate variability at different time scales: a study
699 in the Ebro basin. *Journal of Hydrology* 477: 175-188.

700 Lorenzo-Lacruz J, Vicente-Serrano SM, López-Moreno JI, Beguería S, García-Ruiz JM, Cuadrat JM (2010)
701 The impact of droughts and water management on various hydrological systems in the headwaters of
702 the Tagus River (central Spain). *Journal of Hydrology* 386: 13-26.

703 Lorenzo-Lacruz J, Vicente-Serrano SM, González-Hidalgo JC, López-Moreno JI, Cortesi N (2013)
704 Hydrological drought response to meteorological drought at various time scales in the Iberian
705 Peninsula. *Climate Research* 58: 117-131.

706 Luterbacher J, Schmutz C, Gyalistras D, Xoplaki E, Wanner H (1999) Reconstruction of Monthly NAO and
707 EU Indices Back to 1675. *Geophysical Research Letters* 26: 2745–2748

708 Luterbacher J et al. (2002) Extending North Atlantic Oscillation reconstructions back to 1500. *Atmos Sci*
709 Lett doi:10.1006/asle.2001.004.

710 Luterbacher J, Dietrich D, Xoplaki E, Grosjean M, Wanner H (2004) European seasonal and annual
711 temperature variability, trends, and extremes since 1500. *Science* 303:1499–1503

712 McKee TBN, Doesken J, Kleist J (1993) The relationship of drought frequency and duration to time scales.
713 Eighth Conference on Applied Climatology (American Meteorological Society, Anaheim, CA), pp
714 179–184.

715 Palmer WC (1965) Meteorological droughts. U.S. Department of Commerce Weather Bureau Research
716 Paper 45, 58 pp.

717 Pauling A, Luterbacher J, Casty C, Wanner H (2006) 500 years of gridded high-resolution precipitation
718 reconstructions over Europe and the connection to large-scale circulation. *Climate Dynamics* 26:
719 387-405.

720 Pausas JG (2004) Changes in fire and climate in the eastern Iberian Peninsula (Mediterranean Basin).
721 *Climatic Change* 63: 337-350.

Pokorna L, Huth R (2014) Climate impacts of the NAO are sensitive to how the NAO is defined. *Theor Appl Climatol*, DOI 10.1007/s00704-014-1116-0.

Portis DH, Walsh JE, El Hamly M, Lamb PJ (2001) Seasonality of the North Atlantic Oscillation, *J. Clim.*, 14: 2069–2078.

Potop V, Možný M, Soukup J (2012) Drought evolution at various time scales in the lowland regions and their impact on vegetable crops in the Czech Republic. *Agricultural and Forest Meteorology* 156: 121-133.

Qian B, Corte-Real J, Xu H (2000) Is the North Atlantic Oscillation the most important atmospheric pattern for precipitation in Europe? *Journal of Geophysical Research: Atmospheres* 105: 11901-11910.

Richman MB (1986) Rotation of principal components, *J. Climatol.*, 6, 293– 335.

Santos JF, Portela MM, Pulido-Calvo I (2014) Spring drought prediction based on winter NAO and global SST in Portugal. *Hydrological Processes* 28: 1009-1024.

Schmutz C, Luterbacher J, Gyalistras D, Xoplaki E, Wanner H (2000) Can we trust proxy-based NAO index reconstructions? *Geophys Res Lett* 27(8):1135–1138

Scaini A, Sánchez N, Vicente-Serrano SM, Martínez-Fernández J (2014) SMOS-derived soil moisture anomalies and drought indices: a comparative analysis using in situ measurements. *Hydrological Processes*. DOI: 10.1002/hyp.10150.

Singleton A (2012) Forecasting Drought in Europe with the Standardized Precipitation Index. An assessment of the performance of the European Centre for Medium Range Weather Forecasts. Variable Resolution Ensemble Prediction System. JRC Scientific and Technical Reports. EUR 25254 EN.

Slonosky V, Jones P, Davies T (2000) Variability of the surface atmospheric circulation over Europe, 1774–1995. *Int J Climatol* 20:1875–1897

Slonosky VC, Jones PD, Davies TD (2001) Instrumental pressure observations and atmospheric circulation from the 17th and 18th centuries: London and Paris. *Int J Climatol* 21(3):285–298. doi:10.1002:joc.611

748 Sousa PM et al (2011) Trends and extremes of drought indices throughout the 20th century in the
749 Mediterranean. *Natural Hazards and Earth System Science* 11: 33-51.

750 Trigo RM, Palutikof JP (2001) Precipitation scenarios over Iberia. A comparison between direct GCM
751 output and different downscaling techniques. *Journal of Climate* 14: 4422-4446.

752 Trigo RM, Osborn TJ, Corte-Real JM (2002) The North Atlantic Oscillation influence on Europe: Climate
753 impacts and associated physical mechanisms. *Climate Research* 20: 9-17.

754 Trigo RM, Valente MA, Trigo IF, Miranda PMA, Ramos AM, Paredes D, García-Herrera R (2008) The
755 Impact of North Atlantic Wind and Cyclone Trends on European Precipitation and Significant Wave
756 Height in the Atlantic. *Annals of the New York Academy of Sciences* 1146: 212-234.

757 van der Schrier G, Briffa KR, Jones PD, Osborn TJ (2006) Summer moisture variability across Europe. *J.*
758 *Climate* 19: 2828-2834.

759 Vicente Serrano SM and López-Moreno JI (2006) The influence of atmospheric circulation at different
760 spatial scales on winter drought variability through a semiarid climatic gradient in north east Spain.
761 *International Journal of Climatology* 26: 1427-1456.

762 Vicente-Serrano SM, López-Moreno JI (2008a) The nonstationary influence of the North Atlantic
763 Oscillation on European precipitation. *Journal of Geophysical Research-Atmosphere* 113, D20120,
764 doi:10.1029/2008JD010382.

765 Vicente-Serrano SM, López-Moreno JI (2008b) Differences in the nonstationary influence of the North
766 Atlantic Oscillation on European precipitation under different scenarios of greenhouse gases
767 concentrations. *Geophysical Research Letters* 35, L18710, doi:10.1029/2008GL034832.

768 Vicente-Serrano SM, Beguería S, López-Moreno JI (2010a) A Multi-scalar drought index sensitive to global
769 warming: The Standardized Precipitation Evapotranspiration Index – SPEI. *Journal of Climate* 23:
770 1696-1718.

771 Vicente-Serrano SM, Beguería S, López-Moreno JI, Angulo M, El Kenawy A (2010b) A new global 0.5°
772 gridded dataset (1901-2006) of a multiscalar drought index: comparison with current drought index
773 datasets based on the Palmer Drought Severity Index. *Journal of Hydrometeorology* 11: 1033–1043.

774 Vicente-Serrano SM, Beguería S, López-Moreno JI (2011a) Comment on “Characteristics and trends in
775 various forms of the Palmer Drought Severity Index (PDSI) during 1900-2008” by A. Dai. *Journal of*
776 *Geophysical Research-Atmosphere*. 116, D19112, doi:10.1029/2011JD016410

777 Vicente-Serrano SM et al. (2011b) The NAO impact on droughts in the Mediterranean region. In Vicente-
778 Serrano, S.M., y Trigo, R., (Eds.) *Hydrological, socioeconomic and ecological impacts of the North*
779 *Atlantic Oscillation in the Mediterranean region. Advances in Global Research (AGLO) series.*
780 Springer-Verlag. 23-40.

781 Vicente-Serrano SM, Zouber A, Lasanta T, Pueyo Y (2012a) Dryness is accelerating degradation of
782 vulnerable shrublands in semiarid Mediterranean environments. *Ecological Monographs* 82: 407-
783 428.

784 Vicente-Serrano SM et al. (2012b) Performance of drought indices for ecological, agricultural and
785 hydrological applications. *Earth Interactions* 16: 1–27.

786 Vicente-Serrano SM et al. (2013): The response of vegetation to drought time-scales across global land
787 biomes. *Proceedings of the National Academy of Sciences of the United States of America* 110: 52-
788 57.

789 Vicente-Serrano SM, Van der Schrier G, Beguería S, Azorin-Molina C, Lopez-Moreno JI (2014)
790 Contribution of precipitation and reference evapotranspiration to drought indices under different
791 climates. *Journal of Hydrology*. In press.

792 Wallace JM (2000) North Atlantic Oscillation/annular model: two paradigms-one phenomenon. *Quarterly*
793 *Journal of the Royal Meteorological Society* 126: 791-805.

794 Wanner H et al. (2001) North Atlantic Oscillation—Concepts and studies. *Surv. Geophys.* 22: 321– 382.

795 Wheeler D., García-Herrera R., Wilkinson C.W., Ward C. (2010) Atmospheric circulation and storminess
796 derived from Royal Navy logbooks: 1685 to 1750. *Climatic Change*, 101: 257-280.

797 Wibig J (1999) Precipitation in Europe in relation to circulation patterns at the 500 hPa level. *International*
798 *Journal of Climatology* 19: 253-269. Zveryaev II (2006) Seasonally varying modes in long-term
799 variability of European precipitation during the 20th century. *Journal of Geophysical Research D:*
800 *Atmospheres* 111 (21), D21116.

802 Table 1: Percentage of the variance of the seasonal and annual WI (dependent variable) explained by each
803 one of the five different atmospheric circulation indices (independent variable) for 1950-2008.

804

	<i>Winter</i>	<i>Spring</i>	<i>Summer</i>	<i>Autumn</i>	<i>Annual</i>
<i>NAOi</i>	<i>58.79</i>	<i>20.37</i>	<i>0.09</i>	<i>31.57</i>	<i>40.58</i>
<i>NAO-PC</i>	<i>43.08</i>	<i>0.99</i>	<i>19.28</i>	<i>0.01</i>	<i>6.97</i>
<i>SCAN</i>	<i>8.80</i>	<i>5.60</i>	<i>10.63</i>	<i>5.28</i>	<i>7.48</i>
<i>EA</i>	<i>0.40</i>	<i>10.19</i>	<i>18.93</i>	<i>8.65</i>	<i>9.97</i>
<i>EA-WR</i>	<i>3.26</i>	<i>0.60</i>	<i>6.22</i>	<i>14.50</i>	<i>2.22</i>

805

806

807

Figure captions

Figure 1: Evolution of standardized seasonal and annual NAOi (blue) and WI (red) from 1902 to 2008. The different plots also show the fraction of variance of the WI that can be explained by the NAOi evolution.

Figure 2. Spatial distribution of Pearson's correlation coefficients between the seasonal 3-month SPEI and the seasonal average NAO, WI, NAO-PC, EA, SCAN and EA-WR, and between the summer 9-month SPEI (bottom) and the average 9-month atmospheric circulation indices (right panels). Black lines represent regions with significant correlations ($p < 0.05$).

Figure 3. Spatial distribution of Pearson's correlation coefficients between the seasonal 3-month ETo and the seasonal average NAO, WI, NAO-PC, EA, SCAN and EA-WR, and between the summer 9-month ETo (bottom) and the average 9-month atmospheric circulation indices (right panels). Black lines represent regions with significant correlations ($p < 0.05$).

Figure 4. Spatial distribution of Pearson's correlation coefficients between the seasonal 3-month precipitation and the seasonal average NAO, WI, NAO-PC, EA, SCAN and EA-WR, and between the summer 9-month precipitation (bottom) and the average 9-month atmospheric circulation indices (right panels). Black lines represent regions with significant correlations ($p < 0.05$).

Figure 5. 1950-2008 Pearson's correlation coefficients between the SPEI and the different atmospheric circulation indices in six regions of Europe (shown in the map). The different panels show correlations from the seasonal SPEI calculated at the time-scales of 3-, 6-, 9- and 12-months (columns of each panel). The SPEI time scales were correlated to the six circulation indices also at the time-scales of 3-, 6-, 9- and 12-months (rows of each panel). The values -3, -2, -1 and 0 shown as columns for each time-scale SPEI correspond to seasonal lags with the atmospheric indices. E.g. for winter and a 12-month time-scale of the SPEI, a -3 lag corresponds to correlation of the long-term winter SPEI with the 3-month atmospheric indices of the previous spring, -2 corresponds to the correlation of the long-term winter SPEI with the circulation series of the previous summer at different (3-month and 6-month) time-scales. Non-significant correlations ($p < 0.05$) are in white.

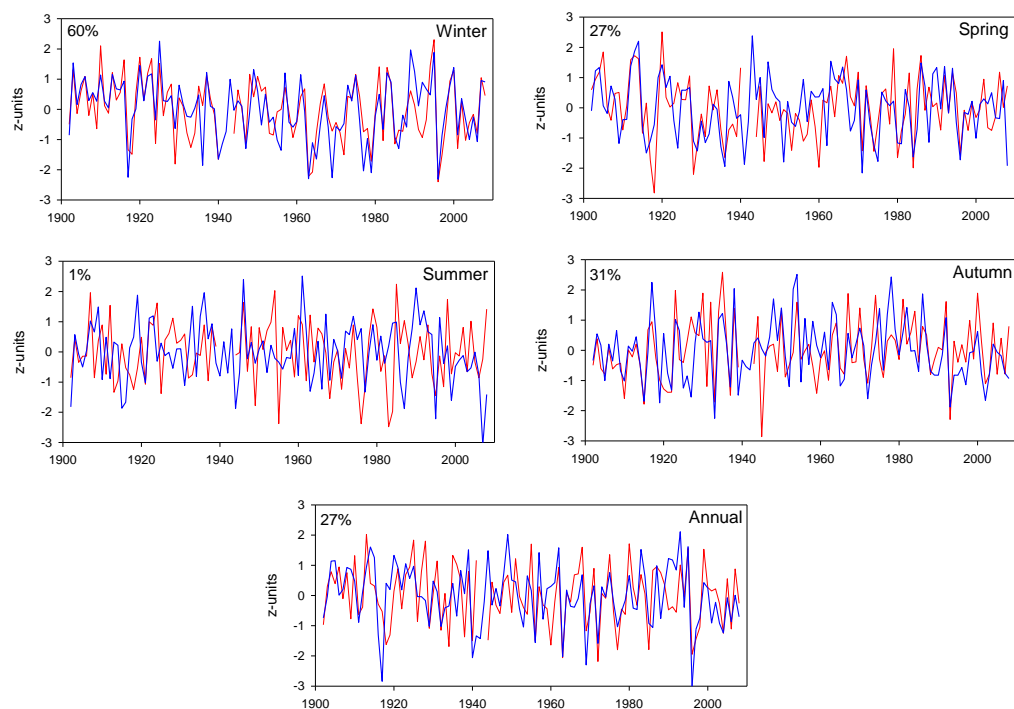
834 Figure 6. Spatial distribution of 1902-2008 Pearson's correlation coefficients between the seasonal 3-month
835 SPEI and the seasonal average NAO and WI (left panels), and between the summer 9-month SPEI
836 (bottom) and the average 9-month NAO and WI (right panels). Black lines represent regions with
837 significant correlations ($p < 0.05$).

838 Figure 7: Relationship between spatial patterns of seasonal and summer long-term correlations between
839 SPEI and WI and NAO in Europe (1902-2008). Solid line represents a perfect agreement between
840 correlation patterns and the dotted line is the linear fit.

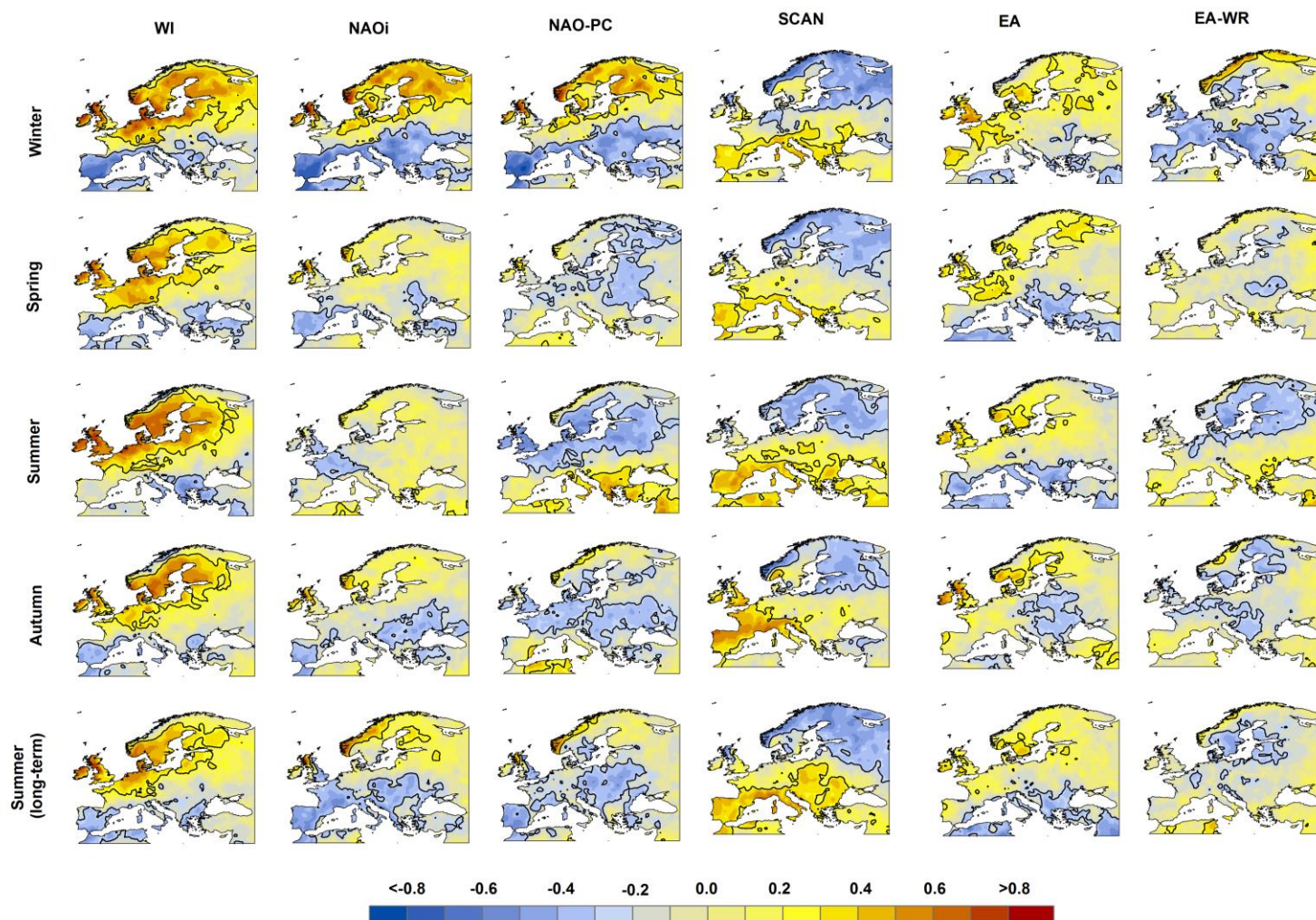
841 Figure 8: Spatial distribution of Pearson's correlation coefficients between the short-term (3-month) winter
842 SPEI and the 3-month winter NAO and WI (two left rows of panels), and between the long-term (9-
843 month) summer SPEI and the 9-month summer NAO and WI (two right rows of panels) for three
844 different periods (1916-1946, 1947-1977, 1978-2008). Black lines represent regions with significant
845 correlations ($p < 0.05$).

846 Figure 9: A) Principal components obtained from the 31-year time series of moving window correlations
847 between the short-term (3-month) winter SPEI and the 3-month winter NAO and WI, and also
848 between the long-term (9-month) summer SPEI and the 9-month summer NAO and WI. B) Spatial
849 distribution of loadings corresponding to the above mentioned components; left/right panels display
850 winter (3-month)/summer (9-month) loadings.

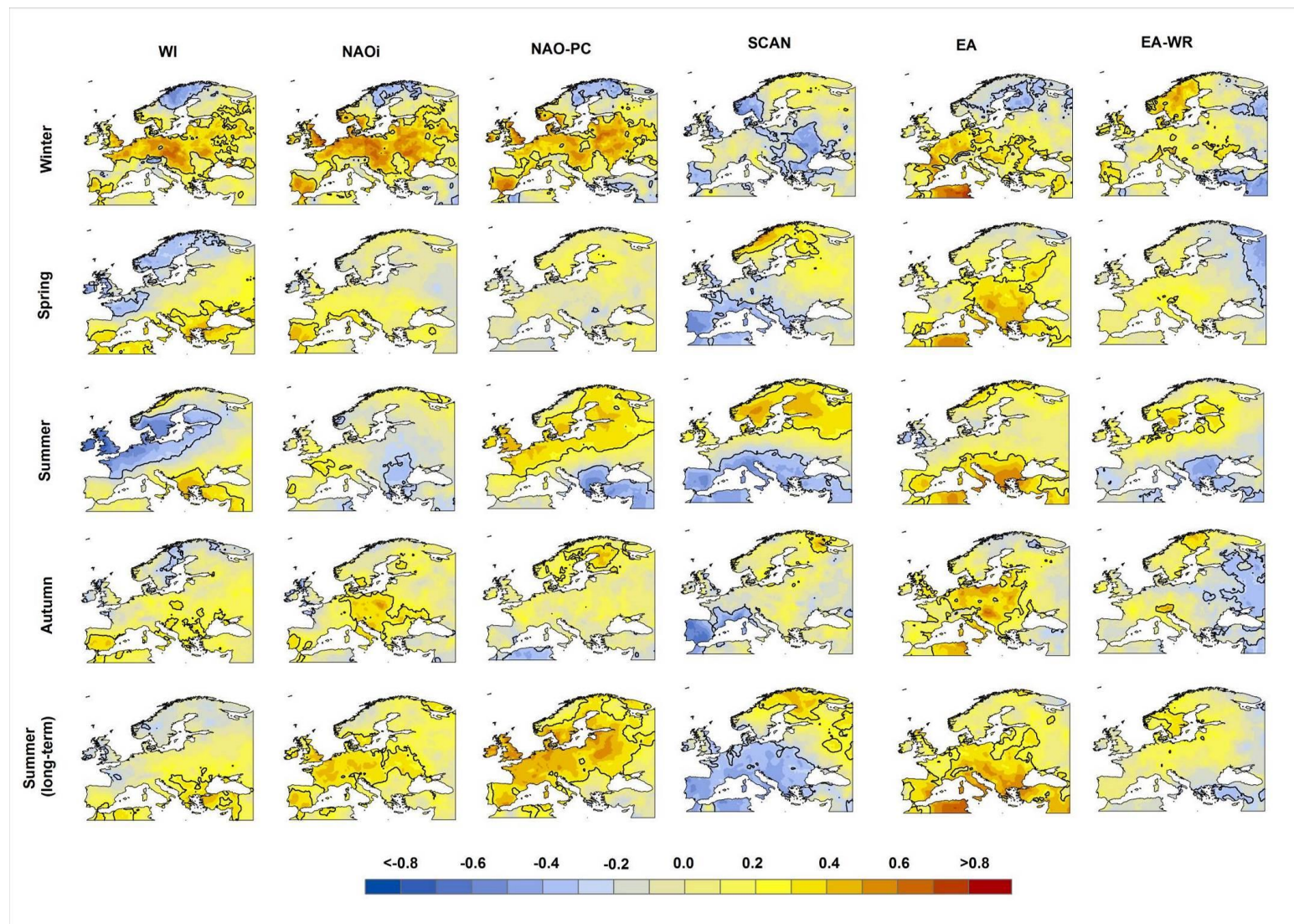
851



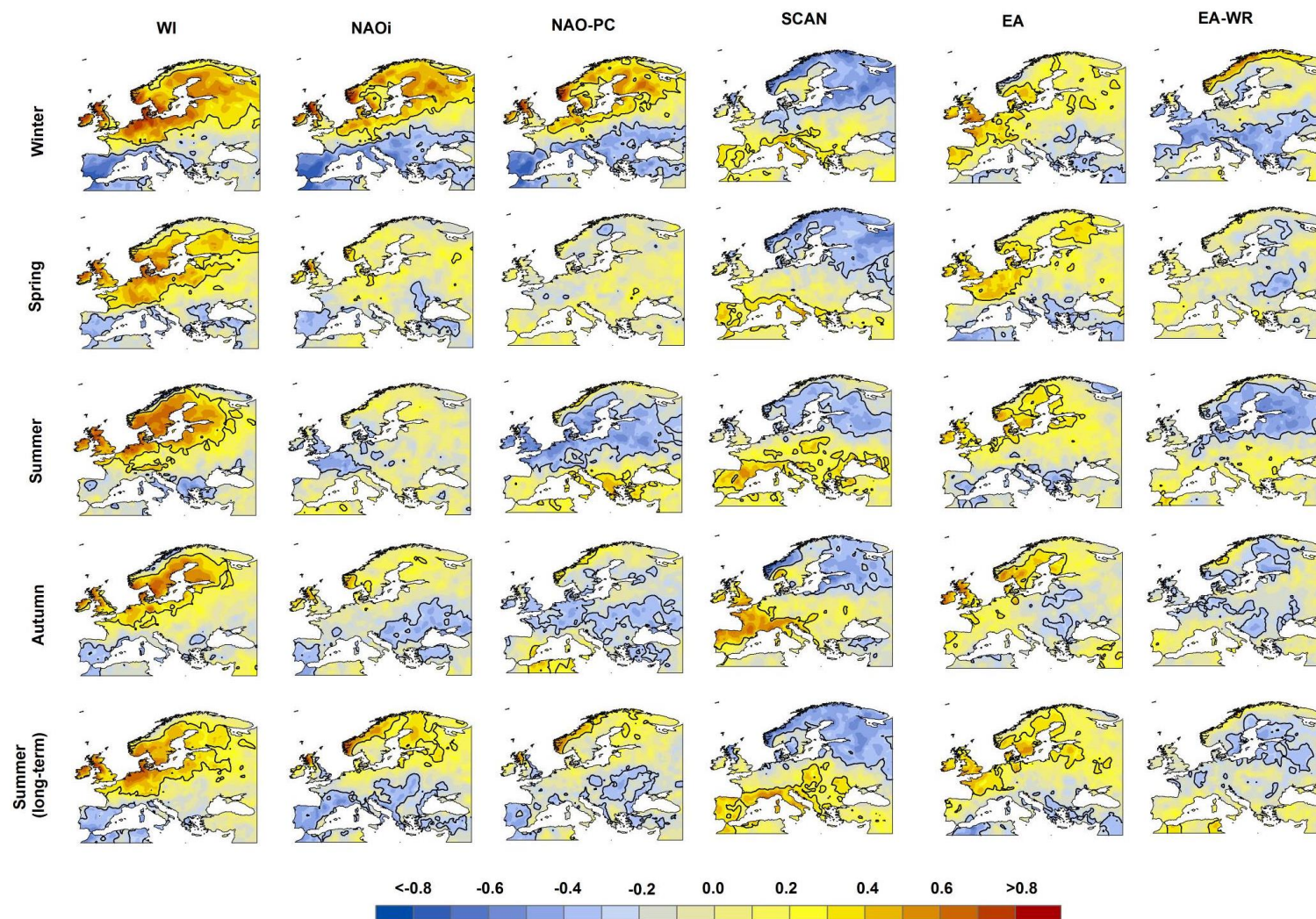
854 Figure 1: Evolution of standardized seasonal and annual NAOi (blue) and WI (red) from 1902 to 2008. The
 855 different plots also show the fraction of variance of the WI that can be explained by the NAOi
 856 evolution.



859 Figure 2. Spatial distribution of Pearson's correlation coefficients between the seasonal 3-month SPEI and the seasonal average NAO, WI, NAO-PC, EA,
 860 SCAN and EA-WR, and between the summer 9-month SPEI (bottom) and the average 9-month atmospheric circulation indices (right panels). Black
 861 lines represent regions with significant correlations ($p < 0.05$).
 862



865 Figure 3. Spatial distribution of Pearson's correlation coefficients between the seasonal 3-month ETo and the seasonal average NAO, WI, NAO-PC, EA, SCAN
866 and EA-WR, and between the summer 9-month ETo (bottom) and the average 9-month atmospheric circulation indices (right panels). Black lines represents
867 regions with significant correlations ($p < 0.05$).



870 Figure 4. Spatial distribution of Pearson's correlation coefficients between the seasonal 3-month precipitation and the seasonal average NAO, WI, NAO-PC,
 871 EA, SCAN and EA-WR, and between the summer 9-month precipitation (bottom) and the average 9-month atmospheric circulation indices (right
 872 panels). Black lines represent regions with significant correlations ($p < 0.05$).

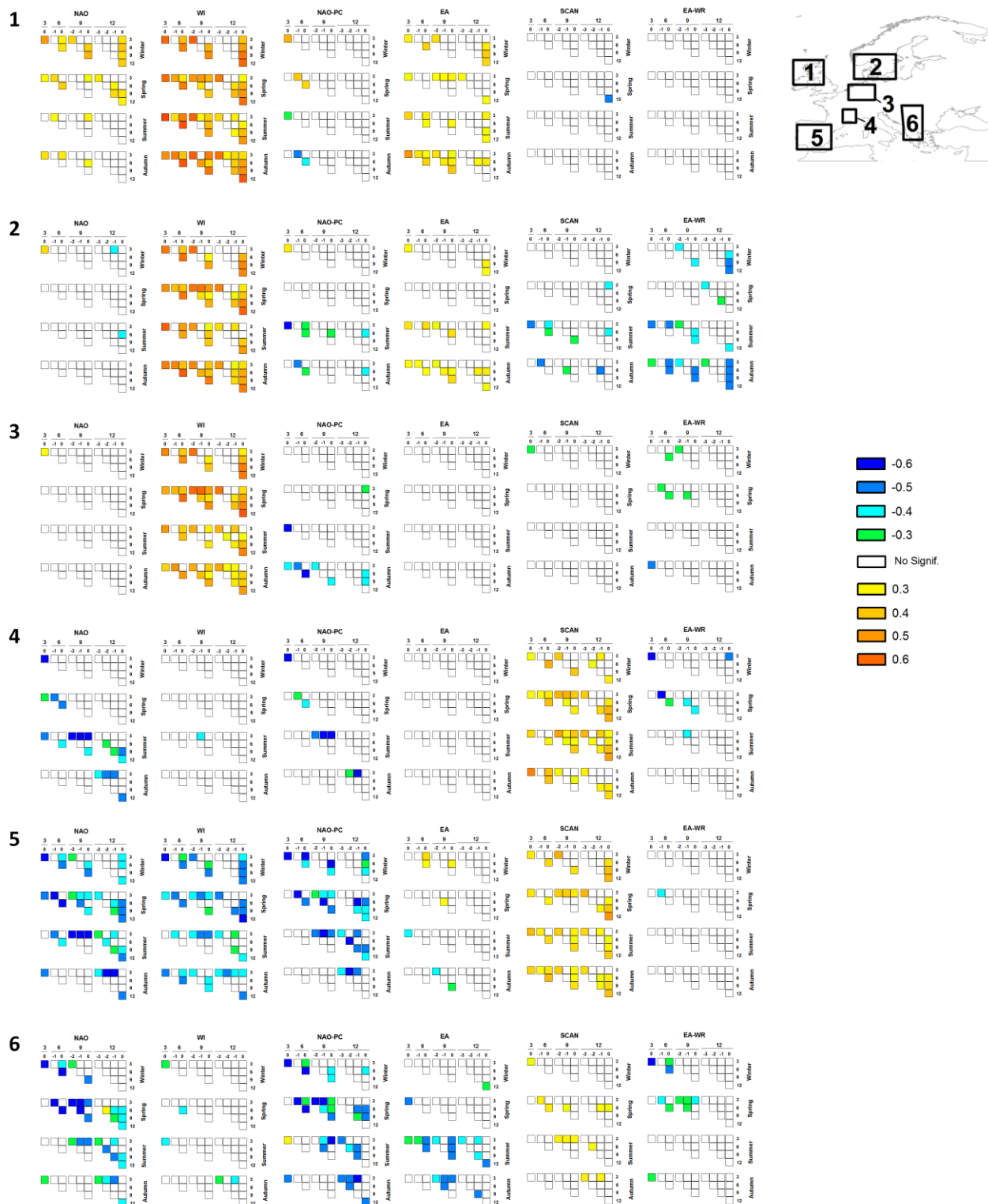
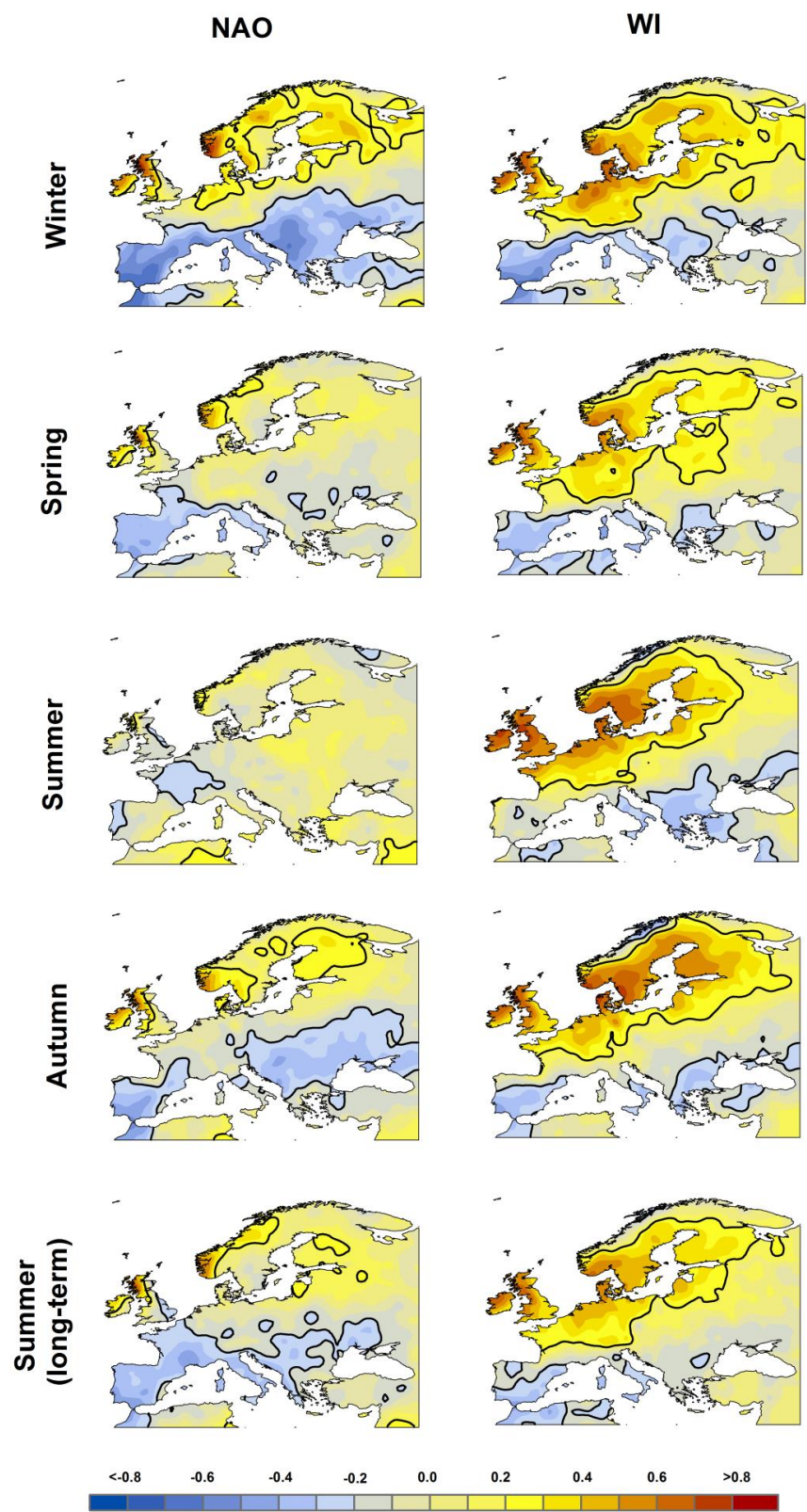


Figure 5. 1950-2008 Pearson's correlation coefficients between the SPEI and the different atmospheric circulation indices in six regions of Europe (shown in the map). The different panels show correlations from the seasonal SPEI calculated at the time-scales of 3-, 6-, 9- and 12-months (columns of each panel). The SPEI time scales were correlated to the six circulation indices also at the time-scales of 3-, 6-, 9- and 12-months (rows of each panel). The values -3, -2, -1 and 0 shown as columns for each time-scale SPEI correspond to seasonal lags with the atmospheric indices. E.g. for winter and a 12-month time-scale of the SPEI, a -3 lag corresponds to correlation of the long-term winter SPEI with the 3-month atmospheric indices of the previous spring, -2 corresponds to the correlation of the long-term winter SPEI with the circulation series of the previous summer at different (3-month and 6-month) time-scales. Non-significant correlations ($p < 0.05$) are in white.



887 Figure 6. Spatial distribution of 1902-2008 Pearson's correlation coefficients between the seasonal 3-month
888 SPEI and the seasonal average NAO and WI (left panels), and between the summer 9-month SPEI (bottom)
889 and the average 9-month NAO and WI (right panels). Black lines represent regions with significant
890 correlations ($p < 0.05$).

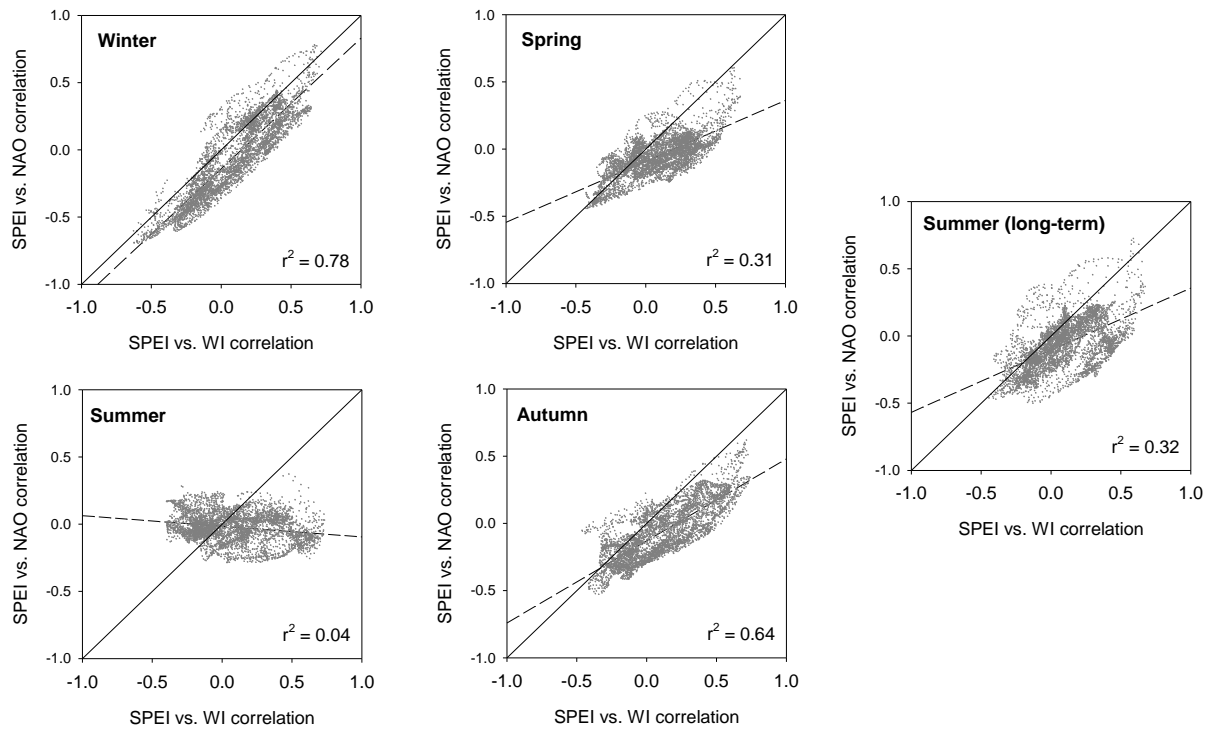
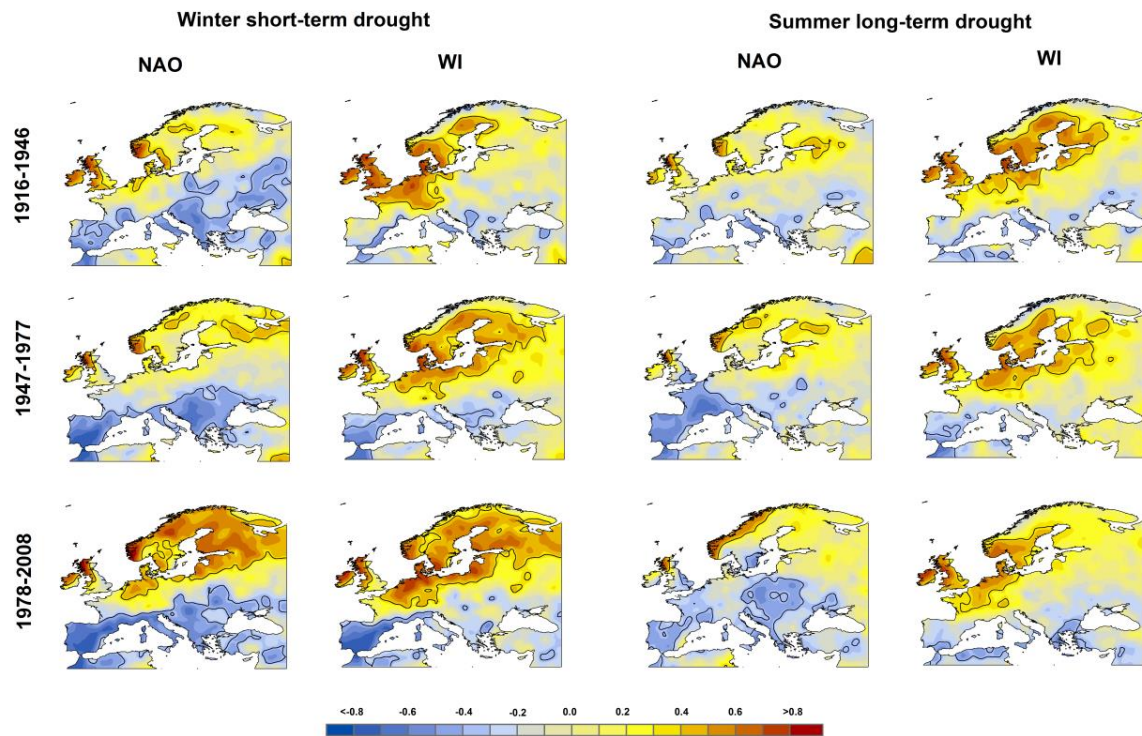


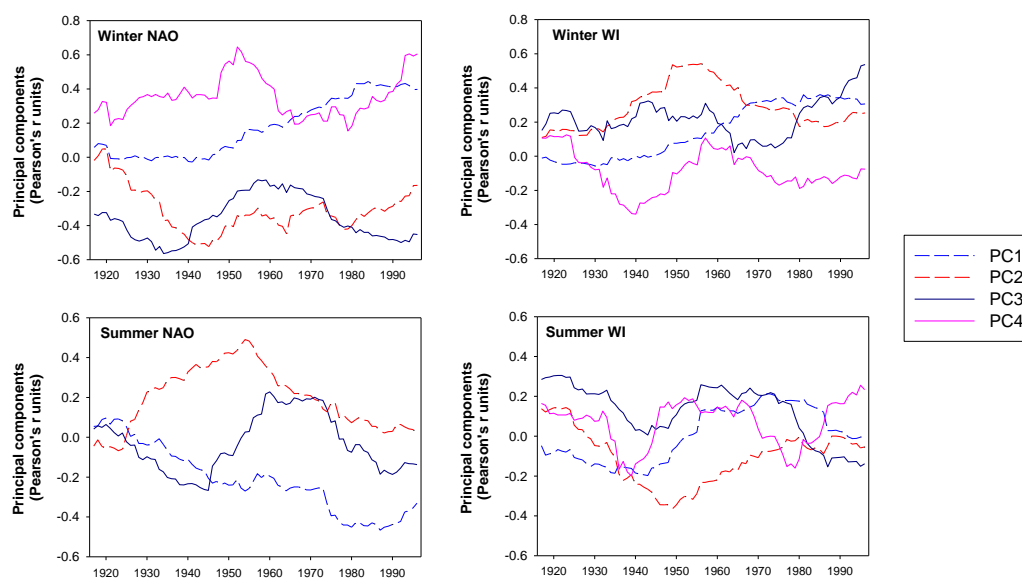
Figure 7: Relationship between spatial patterns of seasonal and summer long-term correlations between SPEI and WI and NAO in Europe (1902-2008). Solid line represents a perfect agreement between correlation patterns and the dotted line is the linear fit.



899 Figure 8: Spatial distribution of Pearson's correlation coefficients between the short-term (3-month) winter
900 SPEI and the 3-month winter NAO and WI (two left rows of panels), and between the long-term (9-
901 month) summer SPEI and the 9-month summer NAO and WI (two right rows of panels) for three
902 different periods (1916-1946, 1947-1977, 1978-2008). Black lines represent regions with significant
903 correlations ($p < 0.05$).
904

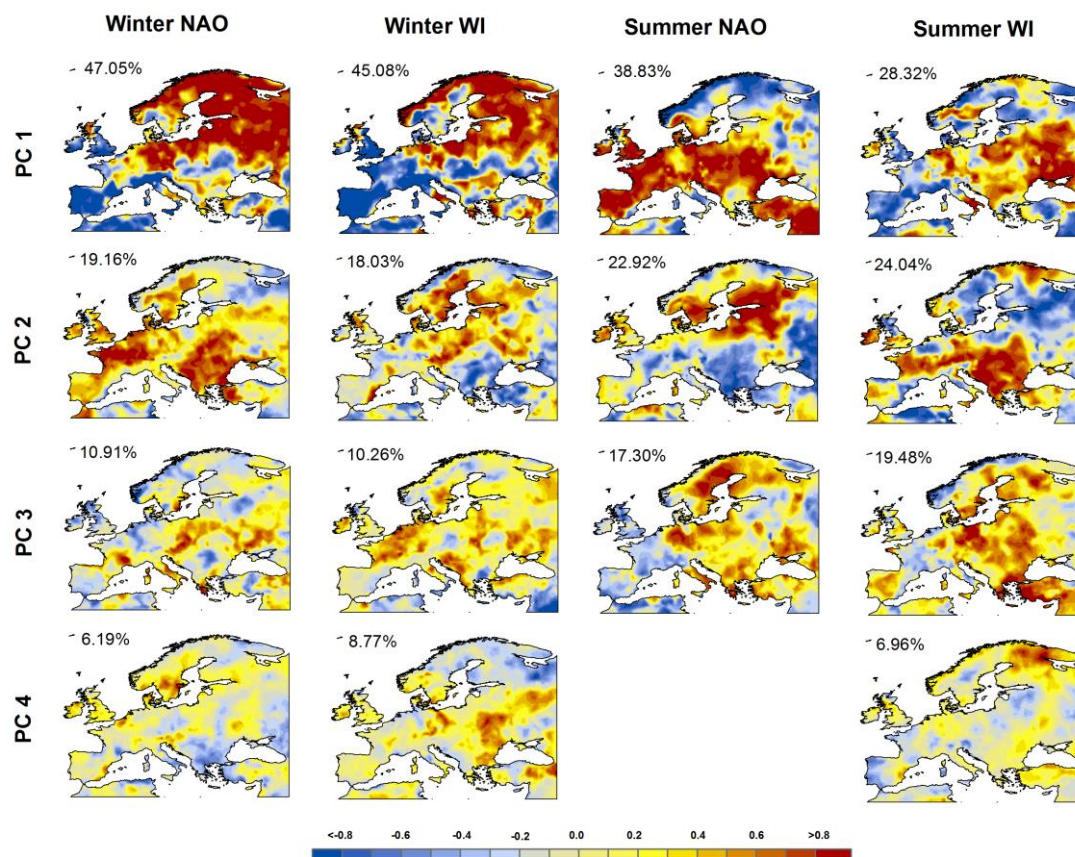
906

907 A)



908

909 B)



910

911 Figure 9: A) Principal components obtained from the 31-year time series of moving window correlations
 912 between the short-term (3-month) winter SPEI and the 3-month winter NAO and WI, and also between the
 913 long-term (9-month) summer SPEI and the 9-month summer NAO and WI. B) Spatial distribution of
 914 loadings corresponding to the above mentioned components; left/right panels display winter (3-
 915 month)/summer (9-month) loadings. The percentage of the total variance explained by the different PCs is
 916 also shown in each plot.